

Electric Supplementary Information

Homochiral hexanuclear nickel(II) metallocyclic structures with high activity for the photocatalytic degradation of organic dyes

Abaid Ullah Malik,^[a] Xia-li Zhou,^[a] Sheng-nan Kong,^[a] Ling-ling Li,^[b] Xiao-li Bao,^[b] and Mou-hai Shu^{*[a]}

^aSchool of Chemistry and Chemical Engineering, Shanghai Jiao Tong University, Shanghai 200240, China

^bInstrumental Analysis Center, Shanghai Jiao Tong University, Shanghai 200240, China

* Corresponding author. Tel: +86-21-54747241; fax: +86-21-54741297.

Email address: mhshu@sjtu.edu.cn

Content	Page
General	S-2
Materials	
Synthesis and characterization	S-3
Synthetic procedure of enantiopure ligands $\mathbf{H}_2\mathbf{L}^{\text{RR}}$ and $\mathbf{H}_2\mathbf{L}^{\text{SS}}$	S-3
Synthetic procedure of enantiopure complexes $\mathbf{1}^{\text{RR}}$ and $\mathbf{1}^{\text{SS}}$	S-4
^1H NMR spectrum of ligand $\mathbf{H}_2\mathbf{L}^{\text{RR}}$	S-5
^{13}C NMR spectrum of ligand $\mathbf{H}_2\mathbf{L}^{\text{RR}}$	S-5
Electrospray mass spectrum (ESI) of ligand $\mathbf{H}_2\mathbf{L}^{\text{RR}}$	S-6
^1H NMR spectrum of ligand $\mathbf{H}_2\mathbf{L}^{\text{SS}}$	S-6
^{13}C NMR spectrum of ligand $\mathbf{H}_2\mathbf{L}^{\text{SS}}$	S-7
Electrospray mass spectrum (ESI) of ligand $\mathbf{H}_2\mathbf{L}^{\text{SS}}$	S-7
Crystal structure figures	S-8~S-10
Vibrational circular dichroism of complexes $\mathbf{1}^{\text{RR}}$ & $\mathbf{1}^{\text{SS}}$	S-11
FT-IR spectrum of ligand $\mathbf{H}_2\mathbf{L}^{\text{RR}}$ and Complex $\mathbf{1}^{\text{RR}}$	S-11
TGA thermogram of complex $\mathbf{1}^{\text{RR}}$	S-12
UV-Vis Spectra of dye degradation control experiment	S-12
Comparison of photocatalytic efficiency of complex $\mathbf{1}^{\text{SS}}$ and TiO_2	S-13
Solid State UV and K-M reflectance plot of complex $\mathbf{1}^{\text{SS}}$	S-14
UV-Vis Spectra of dye degradation for re-use of complex	S-14
UV-Vis spectra of complex before (black) and after (red) irradiation with UV light	S-15
Crystal data and structure refinement for the complex $\mathbf{1}^{\text{RR}}$ and $\mathbf{1}^{\text{SS}}$	S-15
Bond lengths and bond angles of complex $\mathbf{1}^{\text{RR}}$ and $\mathbf{1}^{\text{SS}}$	S-16~S-18
References	S-19

General

All chemicals used were of reagent grade quality purchased from commercial sources and used as such without further purification unless otherwise noted. ^1H and ^{13}C NMR spectra were recorded on a Bruker AVANCE III HD 400 spectrometer at 400 and 100 MHz, respectively. Samples were analysed in DMSO- d_6 at 293 K with TMS as the internal standard unless otherwise specified. HRMS for the ligand and ESI-MS for the complexes were performed on a Waters Micro Mass Q-TOF Premier Mass Spectrometer in negative model, the capillary voltage, source temperature, de-solvation temperature, de-solvation gas, scan range, scan time and inter-scan time are set at 350 °C, 600 l/hr, m/z 100~1500, 1s, and 0.02 s, respectively, and the quoted m/z values are for the major peaks in the isotopic distribution. CD spectra of ligands and complexes were recorded on a JASCO T-815 spectropolarimeter fitted with DRCD apparatus, and the samples were analysed in methanol (HPLC grade), double distilled water or in solid state at room temperature as mentioned in supplementary information. The UV-visible (UV-Vis) absorption spectra were recorded using Lambda 35 UV/Vis Spectrometer (Perkin Elmer, Inc., USA), the samples were analysed in methanol (HPLC Grade) at room temperature. Melting points were measured with SGW X-4 micro melting point apparatus. Thermogravimetric analysis (TGA) was recorded using Pyris 1 TGA, and samples were heated from 50 to 800°C at the rate of 20 °C per minute in nitrogen atmosphere. FT-IR spectra recorded on Perkin-Elmer Paragon 1000 spectrometer in the range of 400~4000 cm^{-1} .

Materials

Commercial compounds used as such without purification

1,4-Phenylenediacetonitrile

L / D-cysteine

Sodium hydrogen carbonate

Sodium hydroxide nickel(II) perchlorate hexahydrate

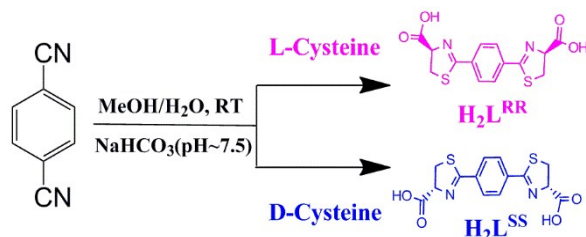
Commercially available solvents used:

Methanol

Acetonitrile

Synthesis and Characterization

General Procedure for Synthesis of Enantiopure Ligands^[1] (H_2L^{RR}/H_2L^{SS}): 1,4-Phenylenediacetonitrile (1.92 g, 15.0 mmol), *L/D*-cysteine (5.45 g, 45.0 mmol) and $NaHCO_3$ (3.78 g, 45.0 mmol) were mixed in a 500 ml in a round bottom flask followed by addition of methanol-water mixture (methanol 250 ml and water 150 ml), and pH was tailored by adding 4N solution of sodium hydroxide to ~ 7.5 and mixture was stirred at room temperature for 48 hours. Methanol was removed by evaporation under reduced pressure (at $40^\circ C$). The small quantity of solid residue was removed by filtration. The clear solution was acidified with hydrochloric acid (2 M) to pH about 2 at $0^\circ C$. The precipitates were collected by filtration and washed with cold water (3×20 ml), dried under vacuum. The product was obtained as white powder with yield about 70 % (**Scheme 1**).



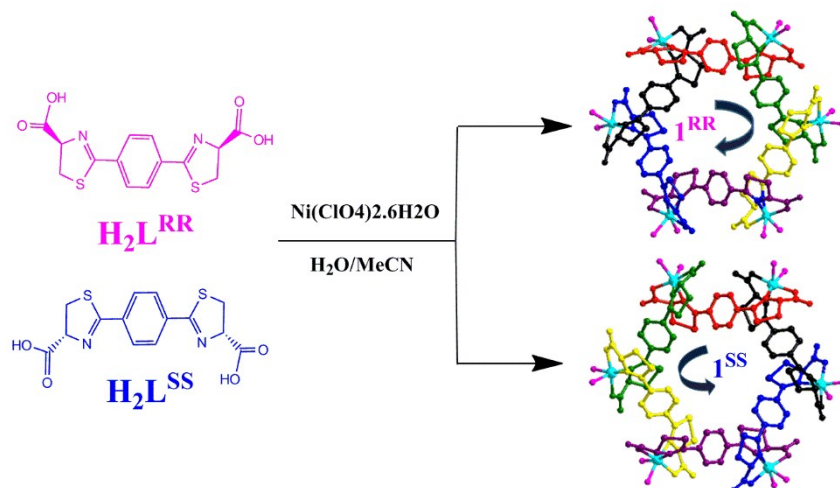
Scheme S1. Synthetic scheme for enantiopure ligands H_2L^{RR} & H_2L^{SS}

H_2L^{RR} : 1H NMR (In $DMSO-d_6$ 400 MHz): δ (ppm) 3.68-3.63 (m, 2H), 3.78-3.73 (m, 2H), 5.34 (t, $J = 8.0$ Hz, 2H), 7.91 (s, 4H), 13.04(s, 2H). (**Fig. S1**): ^{13}C NMR (151 MHz, $DMSO$): $\delta = 172.08, 168.05, 135.32, 129.07, 78.89, 39.52$ ($DMSO$), 35.64ppm. (**Fig. S2**): MS-ESI (m/z): $[M]^-$ (calcd. for $C_{14}H_{11}N_2O_4S_2$: 335.0160). Found: 335.0158, intensity (30%) with some water adducts $[M.H_2O]^-$, $2[M]^-$ 671.0406 (30%), $2[M.H_2O]^-$ and Insource fragments $[M-(CO_2)]^-$ 291.0287(100%), $[M-2(CO_2)]^-$ 247.0376 (50%). (**Fig S3**), Elemental Analysis (%): C, 49.99; H, 3.60; N, 8.33; O, 19.03; S, 19.06; Found C, 49.95; H, 3.62; N, 8.38; O, 19.06; S, 19.04. Melting point $204-205^\circ C$.

H_2L^{SS} : 1H NMR (In $DMSO-d_6$ 400 MHz): δ (ppm) 3.69-3.64 (m, 2H), 3.79-3.74 (m, 2H), 5.35 (t, $J = 8.0$ Hz, 2H), 7.92 (s, 4H), 13.06(s, 2H). (**Fig. S4**): ^{13}C NMR (151 MHz, $DMSO$): $\delta = 178.08, 168.05, 135.2, 129.07, 78.89, 39.52$ ($DMSO$), 35.64ppm. (**Fig. S5**): MS-ESI (m/z): $[M]^-$ (calcd. for $C_{14}H_{11}N_2O_4S_2$: 335.0160). Found: 335.0160. intensity (28%) with some water adducts $[M.H_2O]^-$ and $2[M]^-$ 671.0396 (30%), $2[M.H_2O]^-$ and Insource fragments $[M-(CO_2)]^-$ 291.0281(100%), $[M-2(CO_2)]^-$ 247.0383 (50%). (**Fig S6**), Elemental Analysis (%): C, 49.99; H, 3.60; N, 8.33; O, 19.03; S, 19.06; Found C, 50.05; H, 3.58; N, 8.34; O, 19.10; S, 19.01. Melting point $204-205^\circ C$

General Procedure for synthesis of enantiopure Complexes ($1^{RR}/1^{SS}$)

Enantiopure ligand H_2L^{RR} or H_2L^{SS} 2,2'-(1,4-phenylene)bis(4,5-dihydrothiazole-4-carboxylic acid) (33.6 mg, 0.10 mmol) was dissolved in H_2O (3.0 mL) in a straight test tube followed by the addition of pyridine (dropwise slowly using micro syringe) until the ligand is completely dissolved to get a transparent solution. A solution of $Ni(ClO_4)_2 \cdot 6H_2O$ (54.8 mg, 0.15 mmol) in acetonitrile (1.0 mL) was layered carefully on the above solution. The test tube was covered and kept undisturbed. Greenish blue crystals ($1^{RR}/1^{SS}$) suitable for X-ray diffraction analysis were obtained after a week.



Scheme S2. Synthetic Scheme of Complex 1^{RR} and 1^{SS}

Complex 1^{RR} : Yield 35.2 mg (79% on the basis of ligand's mass).

Complex 1^{SS} : Yield 31.5 mg (71% on the basis of ligand's mass).

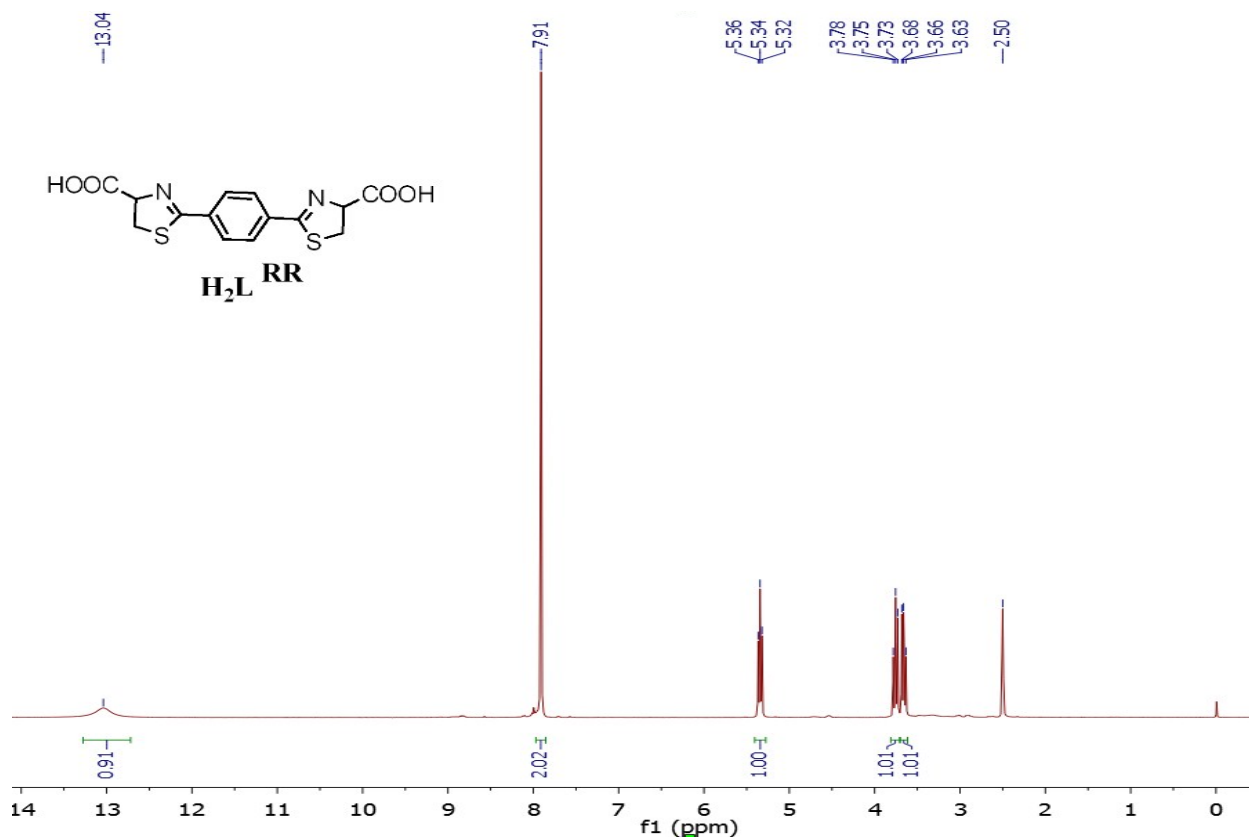


Figure. S1. 1H NMR (DMSO- d_6) Spectrum of Ligand H_2L^{RR} .

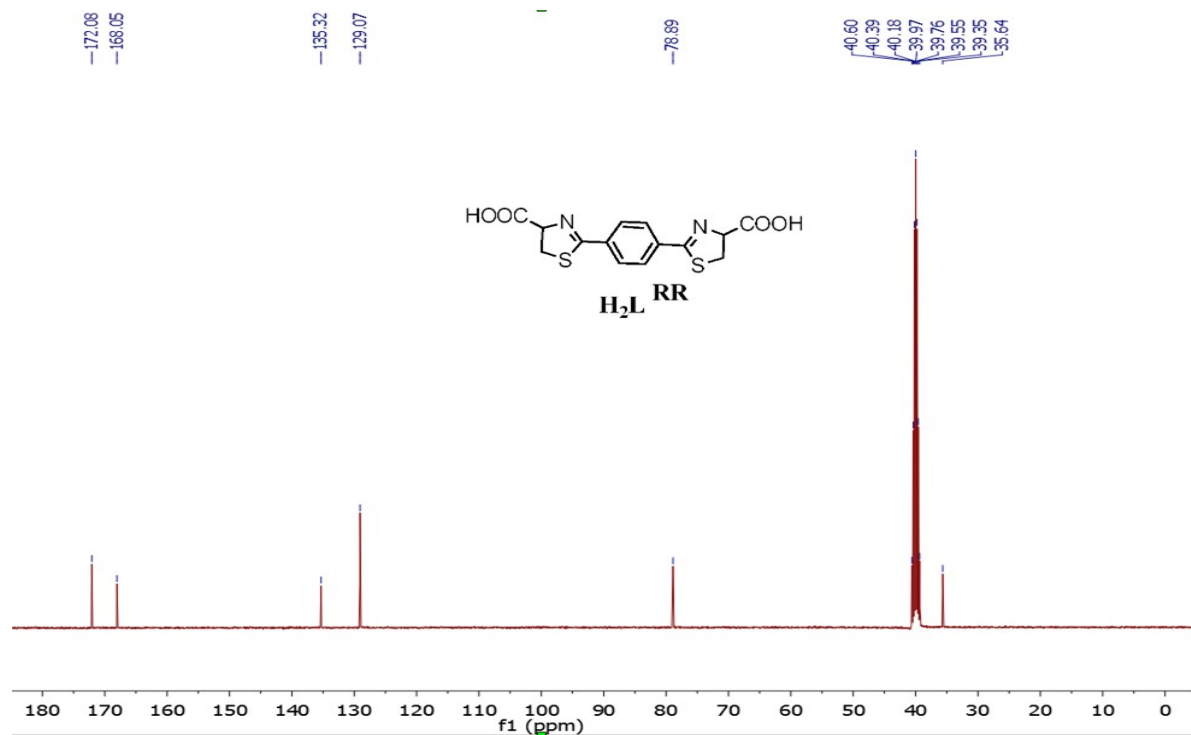


Figure 2. ^{13}C NMR (DMSO- d_6) Spectrum of Ligand H_2L^{RR} .

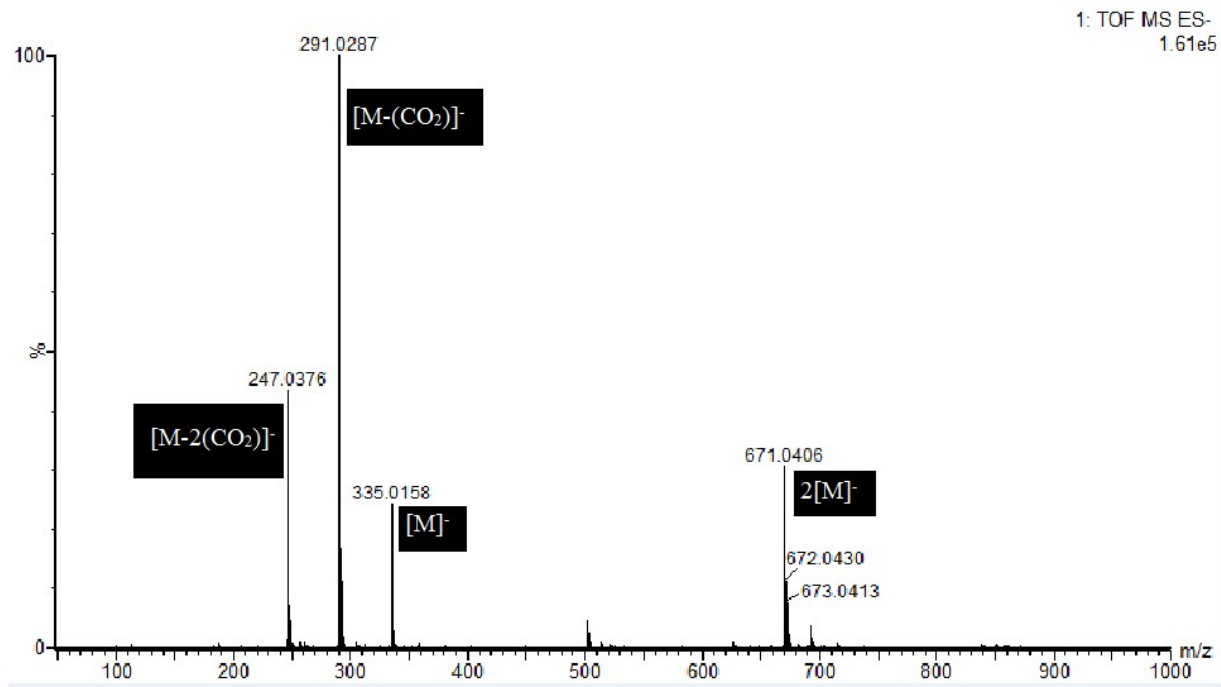


Figure S3. ESI-MS m/z $[M]^-$ spectrum of H_2L^{RR} indicative of water adducts with insource fragmentation $[M-CO_2]^-$ as m/z 291.0287 and $[M-2(CO_2)]^-$ as m/z 247.0376.

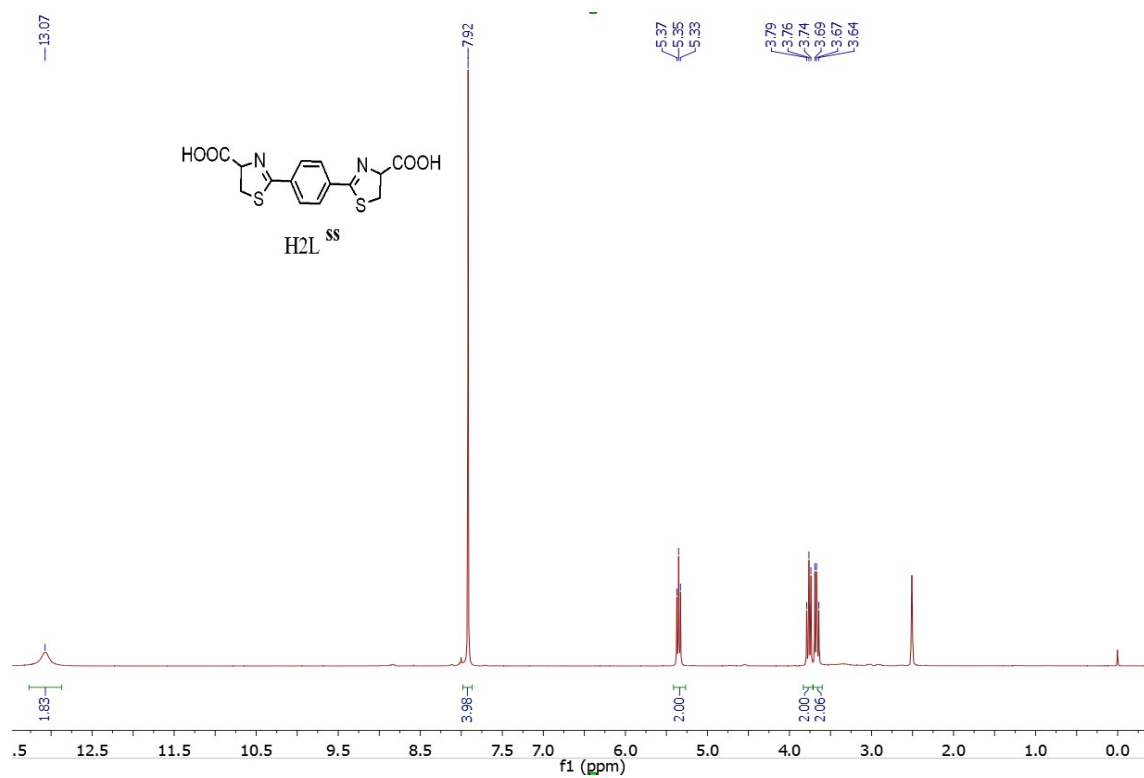


Figure S4. 1H NMR (DMSO- d_6) Spectrum of Ligand H_2L^{SS} .

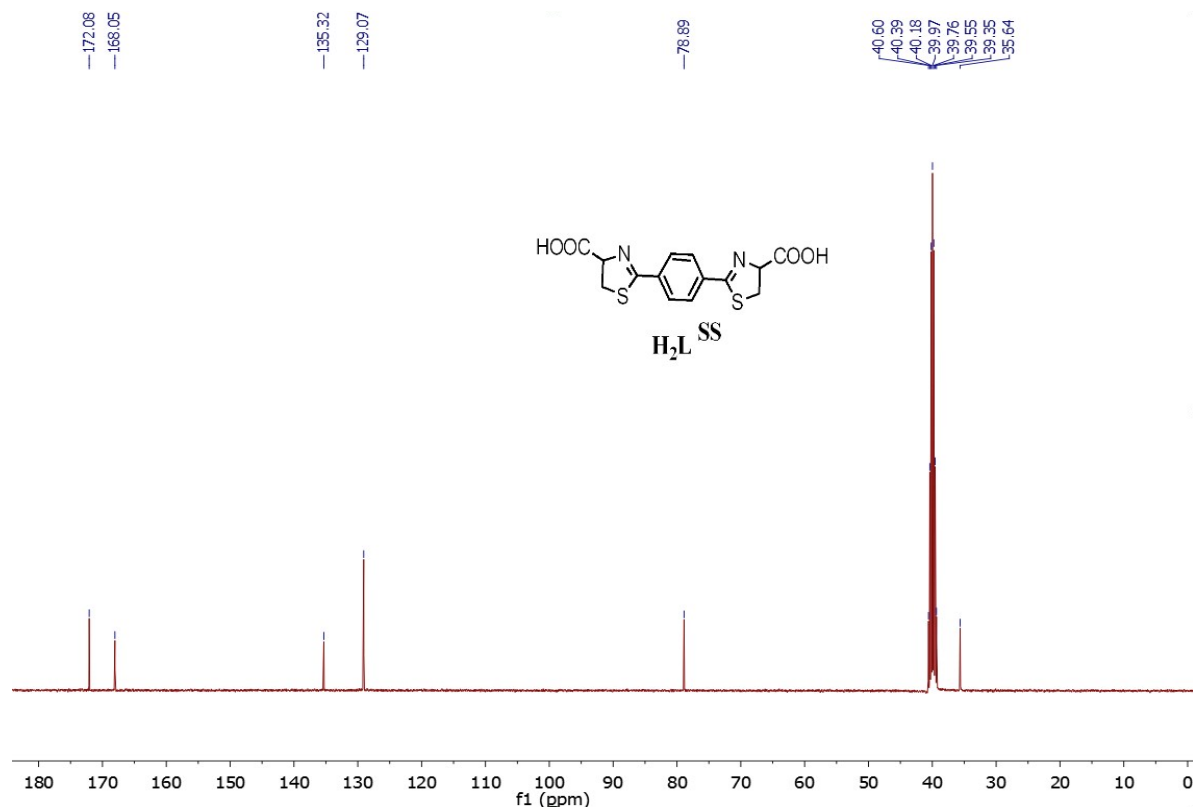


Figure S5. ^{13}C NMR ($DMSO-d_6$) Spectrum of Ligand H_2L^{SS} .

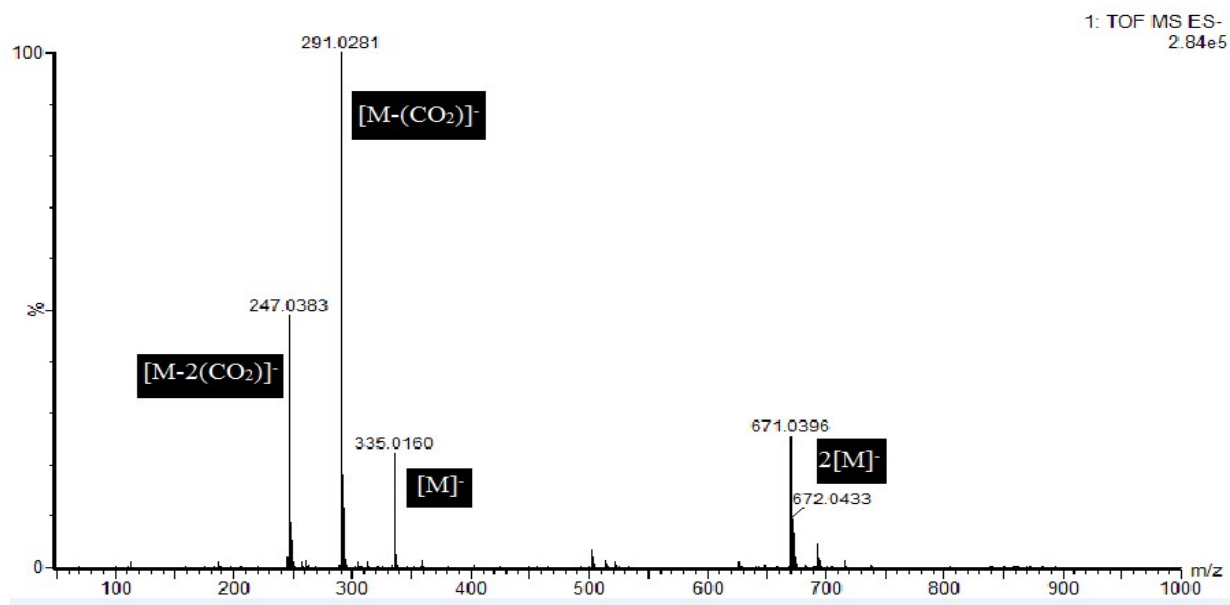


Figure S6. ESI-MS m/z ($M-H$) spectrum of H_2L^{SS} indicative of water adduct with insource ionization fragmentation $[M-CO_2]^-$ as m/z 291.0281 and $[M-2(CO_2)]^-$ as m/z 247.0383.

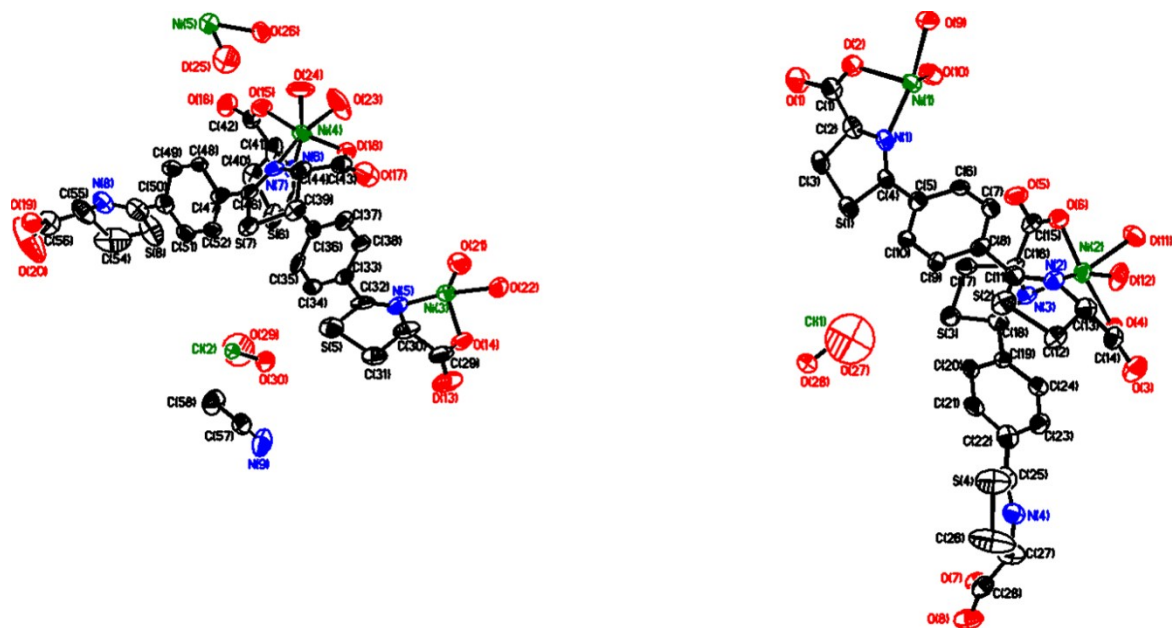


Figure S7a. The minimum unit of complex 1^{RR} , the lattice water molecules and the hydrogen atoms are omitted for clarity.

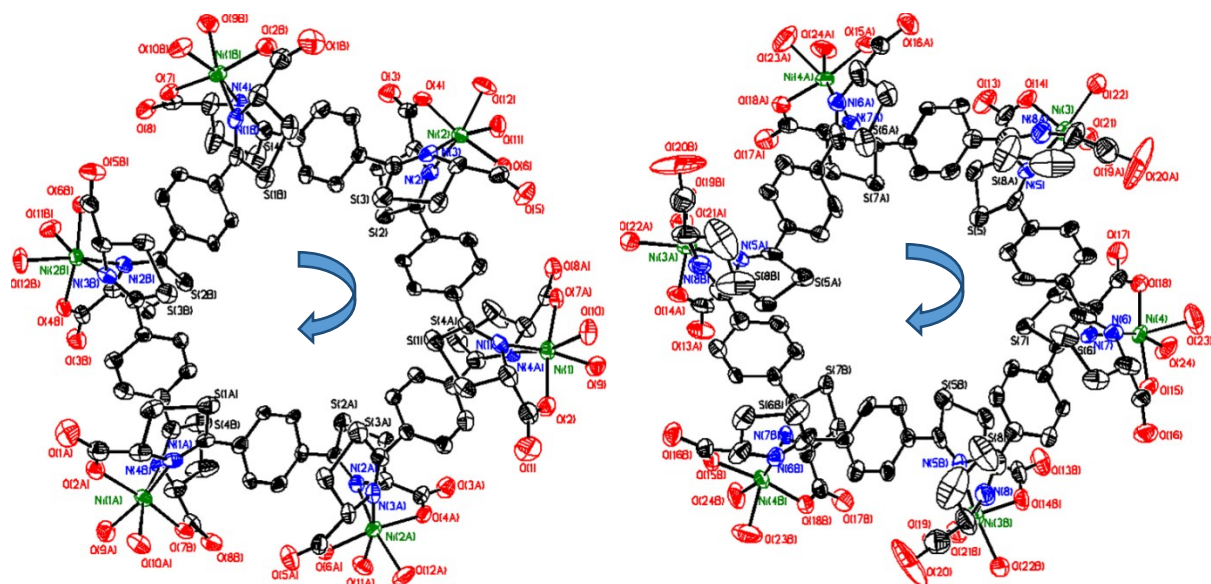


Figure S7b. The Ni_6 -macrocycles in complex 1^{RR} , the hydrogen atoms are omitted for clarity.

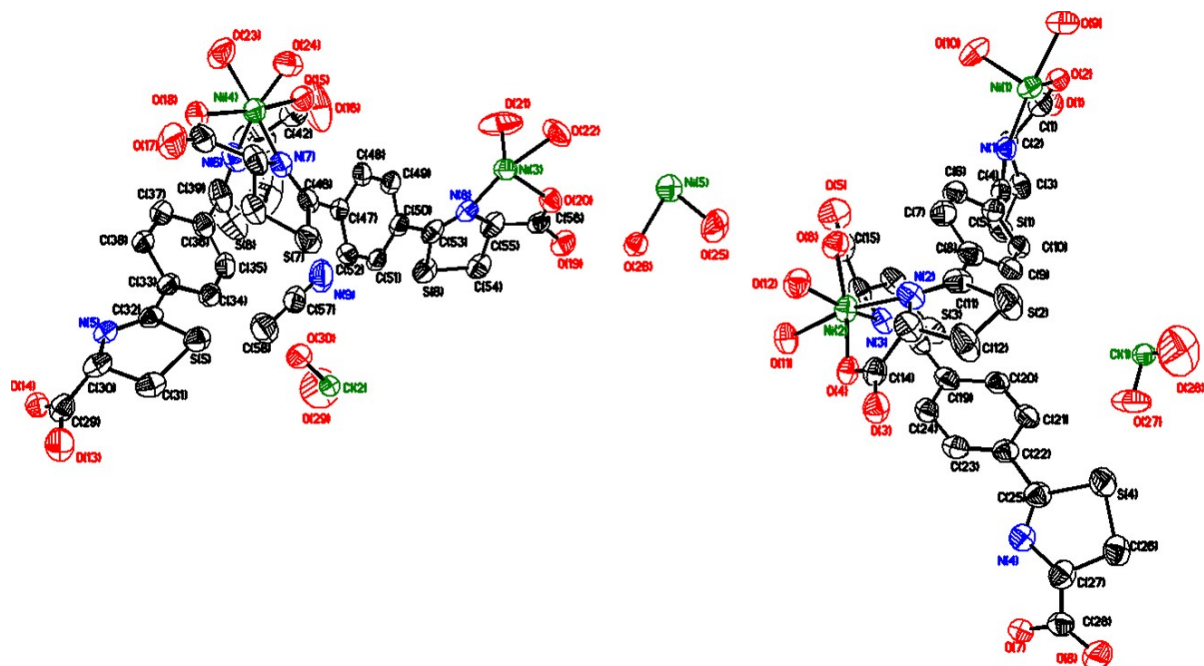


Figure S7c. The minimum unit of complex 1^{SS} , the lattice water molecules and the hydrogen atoms are omitted for clarity.

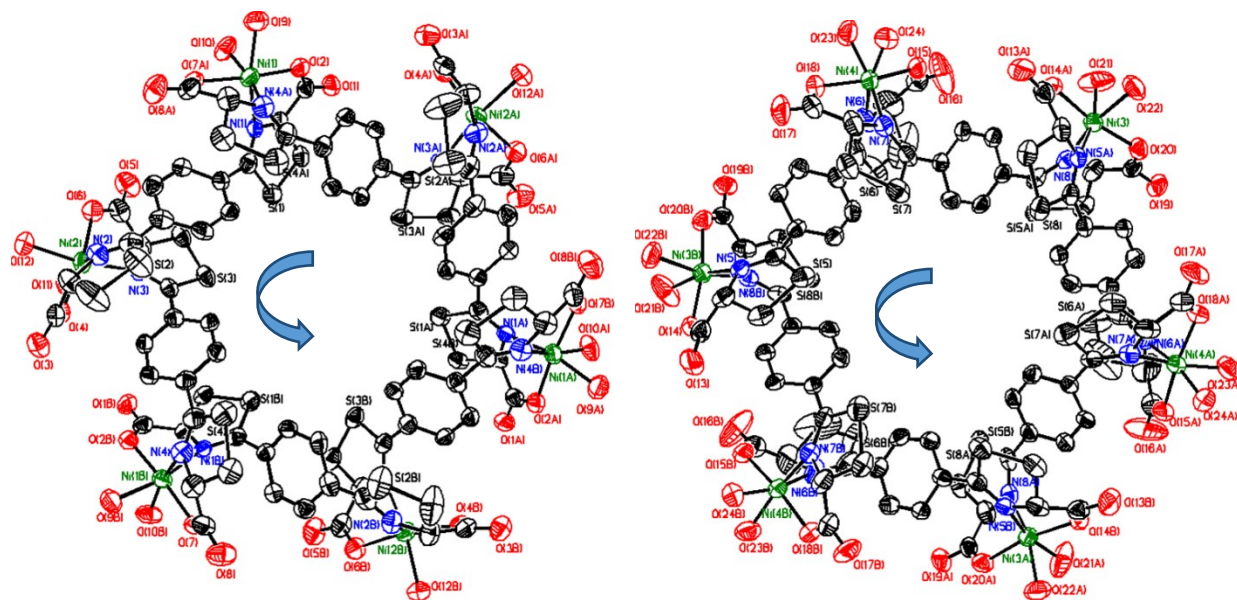


Figure S7d. The Ni_6 -macrocycles in complex 1^{SS} , the hydrogen atoms are omitted for clarity.

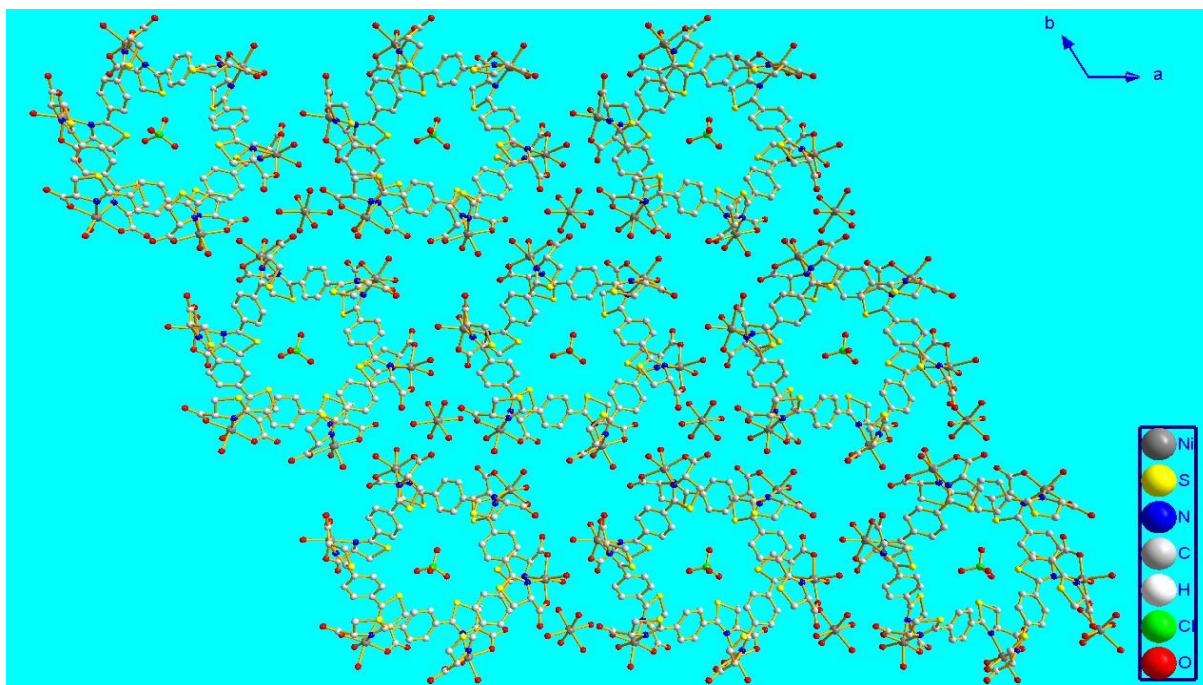


Figure S7e. The pack diagrams of the complex 1^{RR} , the solvent molecules and the hydrogen atoms are omitted for clarity. ClO_4^- Anions are located in the centers of the Ni_6 -rings, there are $[\text{Ni}(\text{H}_2\text{O})_6]^{2+}$ cations out of the Ni_6 -rings.

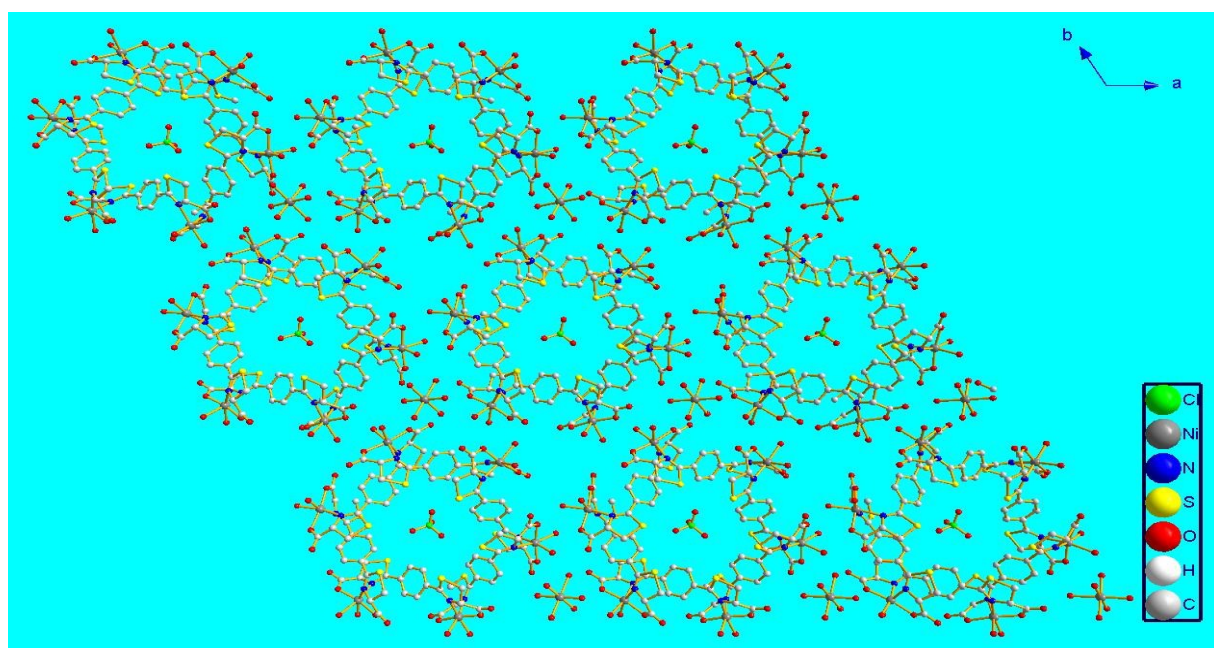


Figure S7f. The pack diagrams of the complex 1^{SS} , the solvent molecules and the hydrogen atoms are omitted for clarity. ClO_4^- Anions are located in the centers of the Ni_6 -rings, there are $[\text{Ni}(\text{H}_2\text{O})_6]^{2+}$ cations out of the Ni_6 -rings.

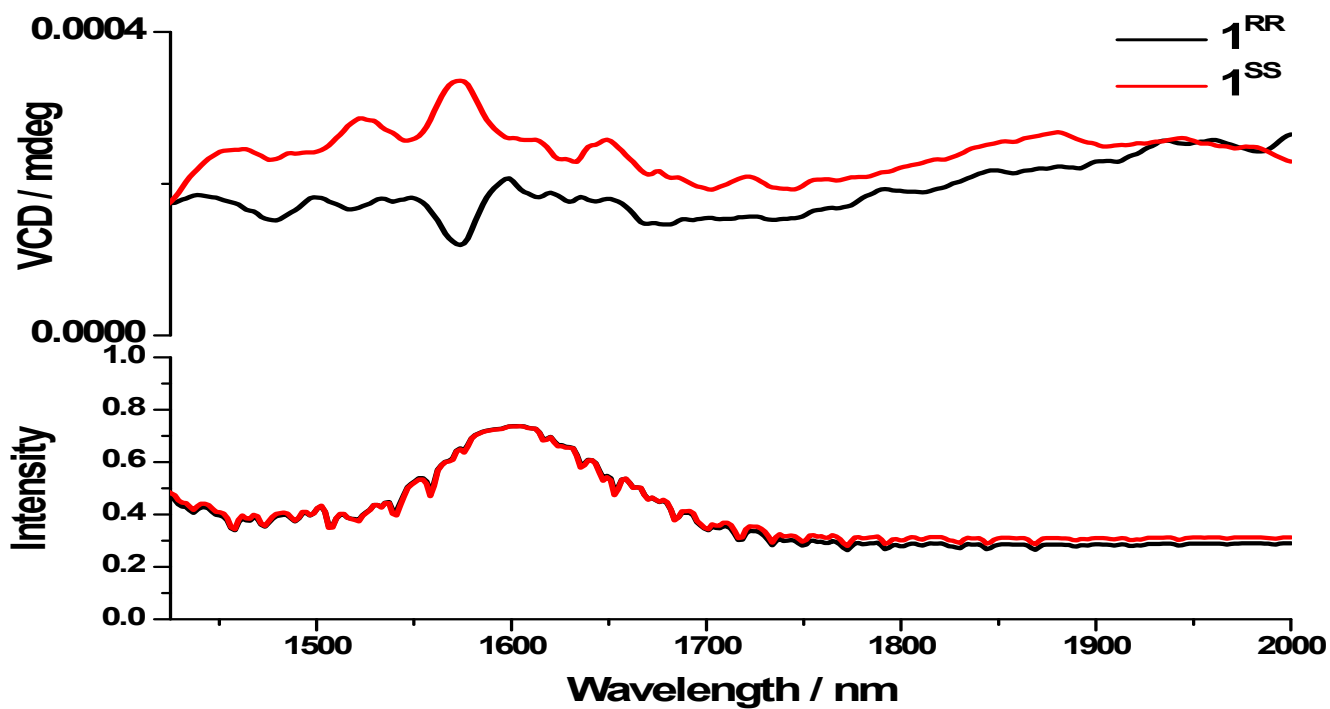


Figure S8. VCD Spectra of Complex 1^{RR} and 1^{SS} (Solid) with KBr. Symmetric behavior is evident for carbonyl functional group moieties^[2] of ligands coordinated in complex 1^{RR} and 1^{SS} .

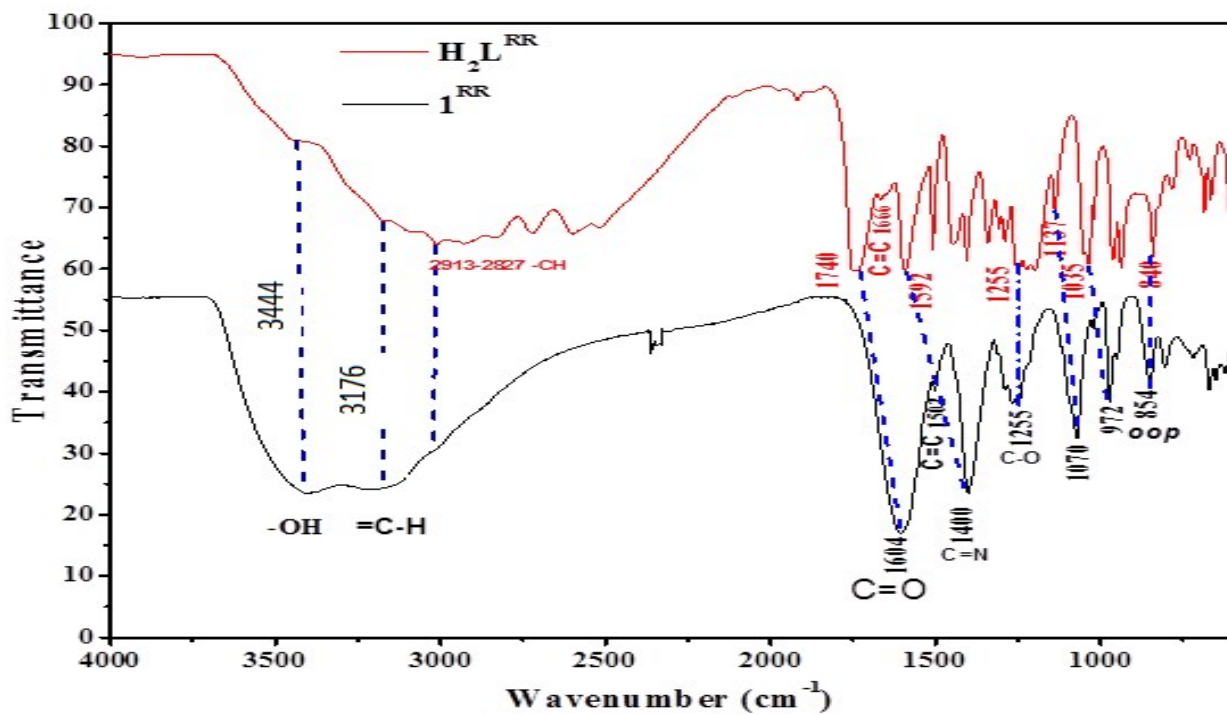


Figure S9. FT-IR spectrum of ligand H_2L^{RR} (Red) and Complex 1^{RR} (Black).

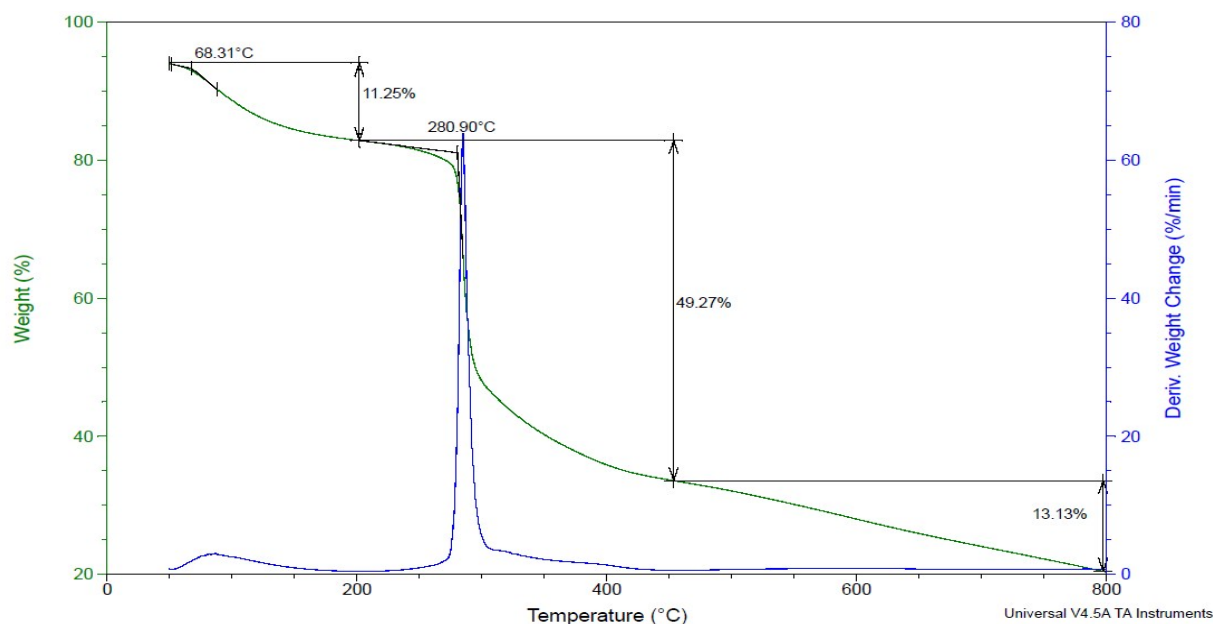
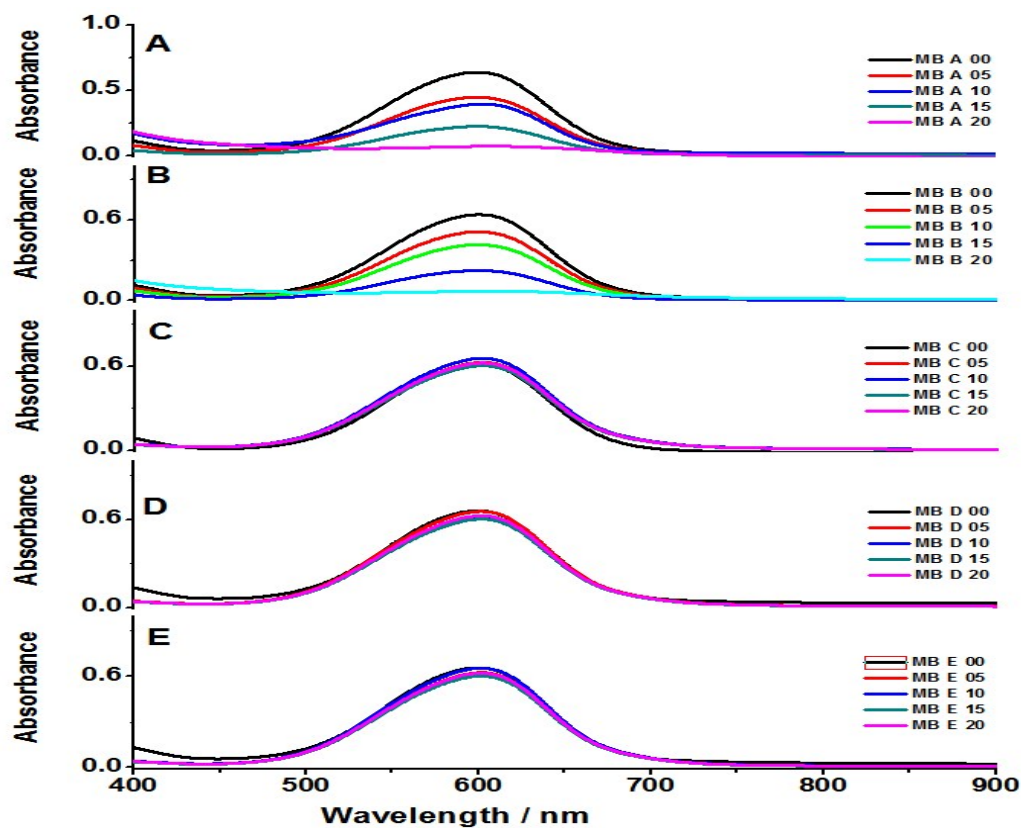


Figure S10. TGA thermogram of complex **1^{RR}**. The first decremented response (weight loss) of approximately 11.5% is probably the removal of adsorbed and coordinated water up to temperature 280°C and second weight loss is continuous weight loss caused by decomposition.



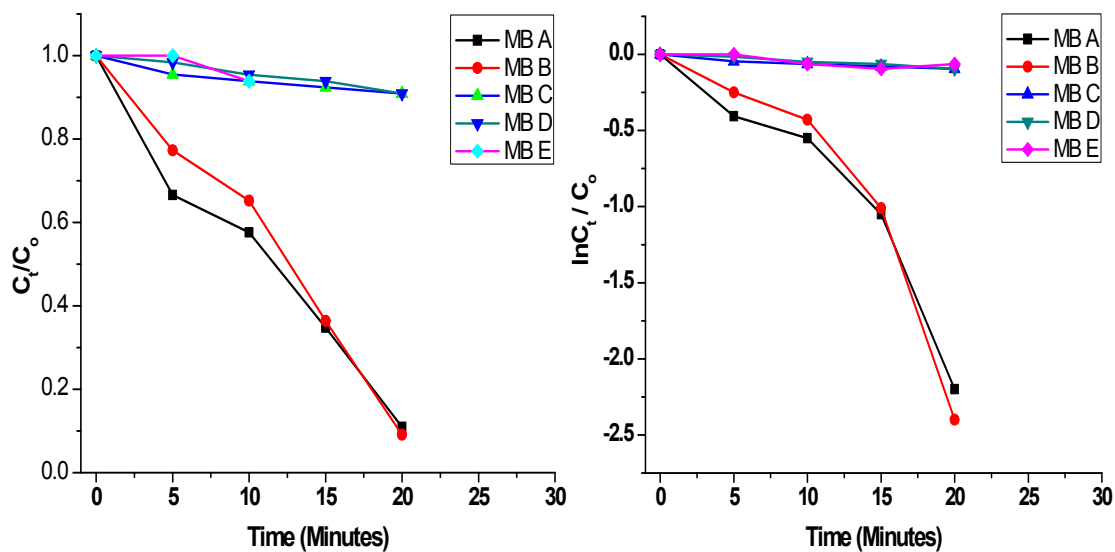


Figure S11. UV plot of dye degradation control experiment of Methylene Blue (aqueous solution) (A) with complex 1^{SS} at sun light, (B) with complex 1^{SS} with UV light, (C) with complex without UV light, (D) with $Ni(ClO_4)_2$ with UV light, (E) only Dye solution

Note: Activity of catalyst can be determined by the decremented UV-Vis absorption of maxima^[3](λ_{max}) and results demonstrated that degradation is mainly driven by the UV-Vis light in presence of photocatalyst 1^{SS} .

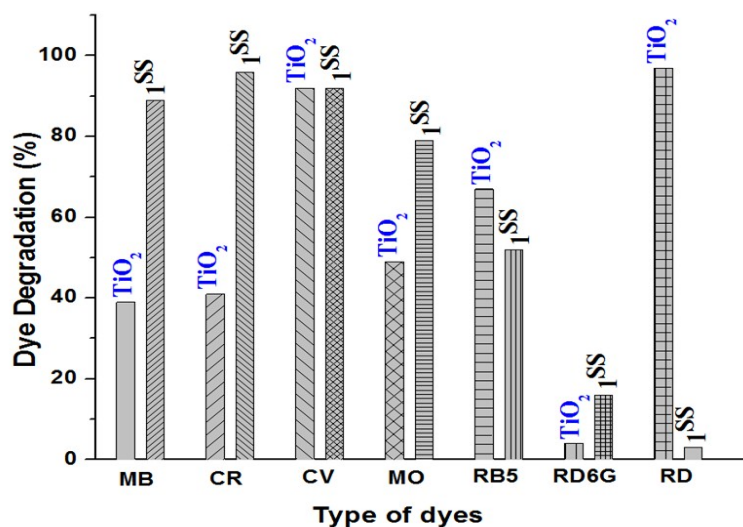


Figure S12. Comparison (%) of photocatalytic efficiency B/W complex 1^{SS} and well-known commercial decolourant (TiO_2) towards degradation of selected organic dyes in aqueous solutions (Concentration $0.01 \text{ mol}\cdot\text{L}^{-1}$).

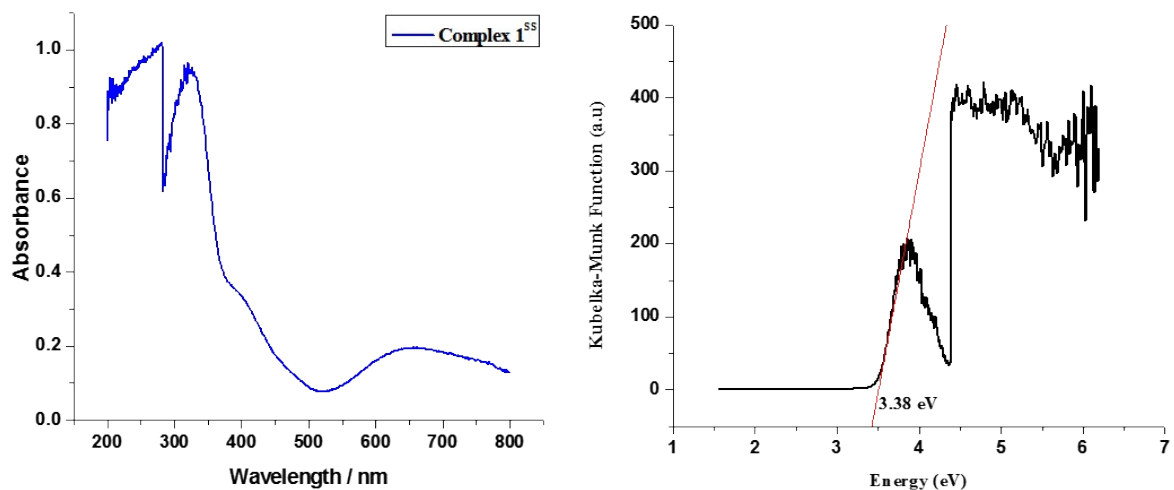


Figure S13 solid State UV plot of complex 1^{SS} (left) (Right) Kubelka–Munk-transformed diffuse reflectance plot of 1^{SS} defined as the intersection point between the energy axis and the line extrapolated from the linear portion of the adsorption edge in a plot of Kubelka–Munk function F versus energy E.^[4]

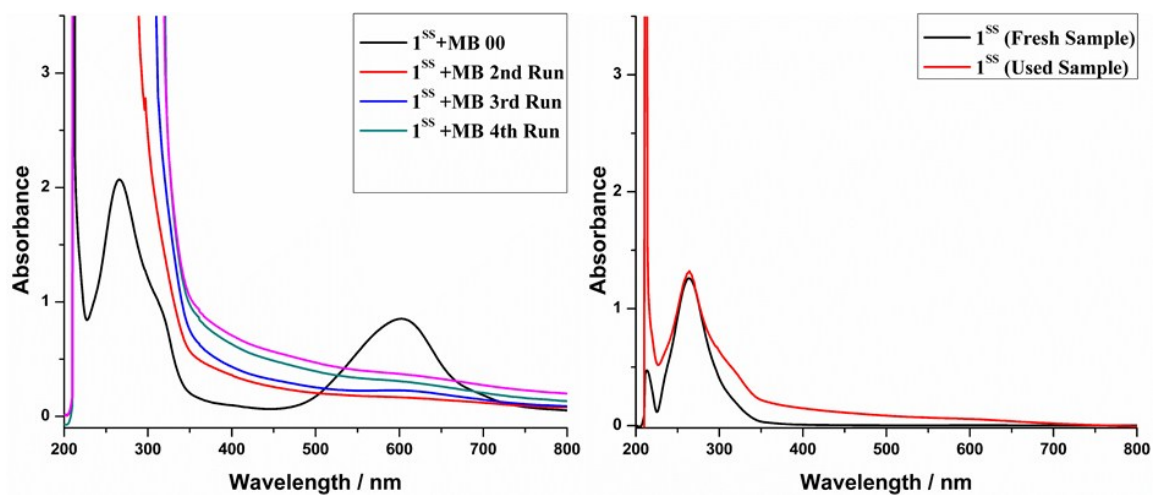


Figure S14. UV-Vis spectra for degradation of methylene blue (MB) up to 4th run (Shows no loss of efficiency but the aggregation effect) (left).

Comparison of UV-Vis spectra of complex 1^{SS} before and after use in dye degradation of MB (right).

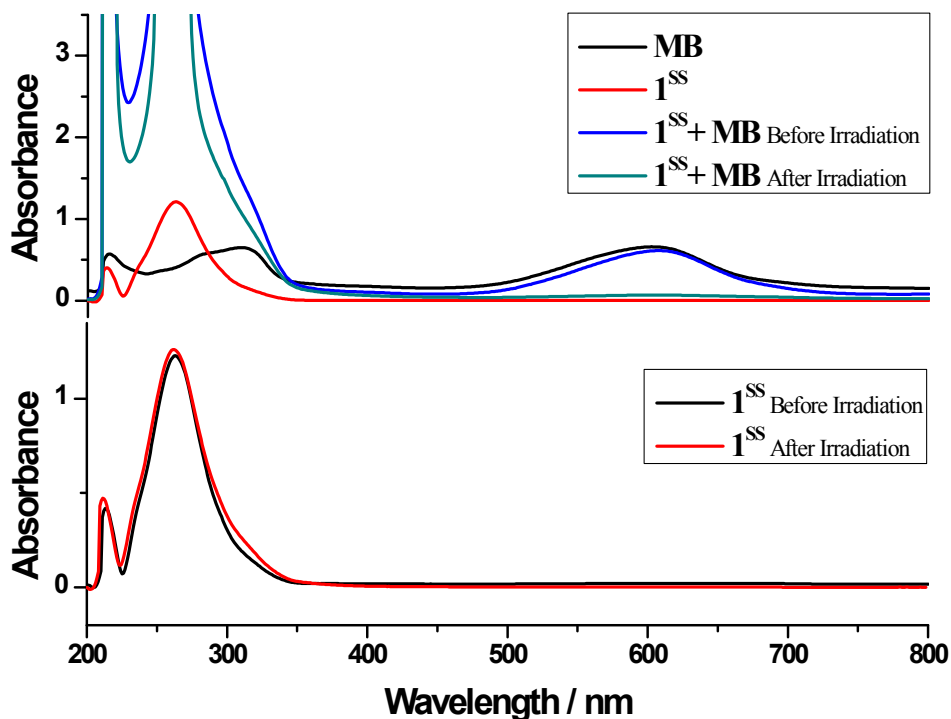


Figure S15 UV-Vis spectra of methylene blue (black), complex 1^{SS} (red), mixture of complex 1^{SS} and MB before irradiation (blue), complex 1^{SS} and MB after irradiation (green) (Up).

UV-Vis spectra of complex before (black) and after (red) irradiation with UV light to see the stability against UV light in solution (Down).

Single crystal structure data and the Structure refinement of the complexes.

The crystals of complexes **1^{RR}** and **1^{SS}** with appropriate dimensions were selected for X-ray single-crystal diffraction. The data were collected on a Bruker SMART APEX II CCD-based X-ray diffractometer with graphite-monochromated Cu-K α radiation ($\lambda = 1.54178 \text{ \AA}$). The multi-scan absorption correction was applied by using the SADABS program [5]. Data collection and reduction were performed using the SMART and SAINT software. Structures were solved by direct methods and refined with full-matrix least-squares on F² using SHELXT-2014[6] and SHELX-2014[7]. Non-hydrogen atoms were refined with anisotropic displacement parameters during the final cycles, the hydrogen atoms of organic ligands were placed in calculated sites and included as riding atoms with isotropic displacement parameters setting to 1.2 \times U_{eq} of the attached C atoms. All the calculations were carried out using SHELXTL programs [6,7]. Due to the relatively weak diffraction, only parts of the hydrogen atoms of coordinated water molecules could be found in difference Fourier maps, therefore all the hydrogen atoms of coordinated water molecules are not introduced. Contributions to scattering due to the highly disordered solvent molecules were removed using the *SQUEEZE* routine of *PLATON*[8], the structures were then refined again using the data generated under SHELX-2014 [7]. The percentage of the weight loss of the removed solvents in complex **1^{RR}** is $(6182.08-5454.19) / 6182.08 = 11.77\%$, the value is closed to the result of TGA (ca. 11.25% weight loss before 200 °C, Fig S10). The crystallographic data and structure refinement details of the complexes **1^{RR}** and **1^{SS}** are

summarized in **Table S1**. Selected bond lengths and angles of complexes **1^{RR}** and **1^{SS}** are listed in **Table S2**.

Table S1. Crystal data and structure refinement of Complexes **1^{RR}** and **1^{SS}**

	Complex 1^{RR}	Complex 1^{SS}
Empirical formula	C ₁₆₈ H ₁₂₀ Cl ₂ N ₂₄ Ni ₁₃ O ₈₆ S ₂₄	C ₁₆₈ H ₁₂₀ Cl ₂ N ₂₄ Ni ₁₃ O ₈₆ S ₂₄
Formula weight	5454.19	5454.19
Temperature (K)	150(2)	173(2)
Wavelength (Å)	1.54178	1.54178
Crystal system	Hexagonal	Hexagonal
Space group	P6(3)	P6(3)
a (Å)	20.5163(2)	20.5789(5)
b (Å)	20.5163(2)	20.5789(5)
c (Å)	38.7061(9)	38.9048(13)
α (°)	90	90
β (°)	90	90
γ (°)	120	120
Volume (Å ³)	14109.4(4)	14268.5(8)
Z	2	2
Density (calculated) (g/cm ³)	1.284	1.270
Absorption coefficient (mm ⁻¹)	3.389	3.352
F(000)	5532	5532
Crystal size (mm ³)	0.28 × 0.26 × 0.18	0.38 × 0.32 × 0.22
Theta range for data collection(°)	2.28 to 68.26	2.48 to 68.002
	-24 ≤ h ≤ 24	-24 ≤ h ≤ 24
Index ranges	-23 ≤ k ≤ 24	-24 ≤ k ≤ 24
	-33 ≤ l ≤ 46	-46 ≤ l ≤ 46
Reflections collected	84357	96852
Independent reflections	14385 [R(int) = 0.0527]	16342 [R(int) = 0.0446]
Data / restraints / parameters	14385 / 976 / 952	16342 / 976 / 952
Goodness-of-fit on F2	1.043	1.032
Final R indices [I > 2σ(I)]: R ₁ , wR ₂	0.0673, 0.1896	0.0756, 0.2150
R indices (all data): R ₁ , wR ₂	0.0828, 0.2022	0.0854, 0.2278
Absolute structure parameter	0.081(8)	0.072(7)
Largest diff. peak and hole (e.Å ⁻³)	1.065 and -0.490	1.504 and -0.697

Table S2. Selected bond distances (Å) and angles (°) of the complexes **1^{RR}** and **1^{SS}**

Complex 1^{RR}			
Ni(1)-O(2)	2.038(7)	Ni(1)-O(10)	2.121(8)
Ni(1)-O(7)#1	2.039(6)	Ni(1)-N(1)	2.116(7)
Ni(1)-O(9)	2.058(7)	Ni(1)-N(4)#1	2.114(9)
Ni(2)-O(4)	2.052(7)	Ni(2)-O(6)	2.067(6)
Ni(2)-O(11)	2.103(8)	Ni(2)-O(12)	2.055(7)
Ni(2)-N(2)	2.106(8)	Ni(2)-N(3)	2.131(8)
Ni(3)-O(14)	2.044(8)	Ni(3)-O(21)	2.092(11)
Ni(3)-O(22)	2.068(10)	Ni(3)-O(19)#2	2.063(10)
Ni(3)-N(5)	2.112(11)	Ni(3)-N(8)#2	2.151(13)
Ni(4)-O(15)	1.982(7)	Ni(4)-O(18)	2.036(8)
Ni(4)-O(23)	2.113(11)	Ni(4)-O(24)	2.085(10)
Ni(4)-N(7)	2.076(8)	Ni(4)-N(6)	2.106(10)
Ni(5)-O(25)	2.087(10)	Ni(5)-O(26)	2.074(9)
Ni(5)-O(26)#3	2.074(9)	Ni(5)-O(26)#4	2.074(9)
Ni(5)-O(25)#3	2.087(10)	Ni(5)-O(25)#4	2.087(10)
O(2)-Ni(1)-O(7)#1	171.8(3)	O(9)-Ni(1)-N(1)	166.2(3)
O(2)-Ni(1)-O(9)	87.7(3)	N(4)#1-Ni(1)-N(1)	94.4(3)
O(7)#1-Ni(1)-O(9)	84.3(3)	O(2)-Ni(1)-O(10)	90.8(3)
O(2)-Ni(1)-N(4)#1	103.8(3)	O(7)#1-Ni(1)-O(10)	87.6(3)
O(7)#1-Ni(1)-N(4)#1	78.3(3)	O(9)-Ni(1)-O(10)	89.2(3)
O(9)-Ni(1)-N(4)#1	93.8(3)	N(4)#1-Ni(1)-O(10)	165.2(3)
O(2)-Ni(1)-N(1)	79.6(3)	N(1)-Ni(1)-O(10)	85.6(3)
O(7)#1-Ni(1)-N(1)	108.3(3)	O(4)-Ni(2)-O(12)	86.2(3)
O(4)-Ni(2)-O(6)	171.6(3)	O(6)-Ni(2)-N(2)	108.6(3)
O(12)-Ni(2)-O(6)	85.4(3)	O(11)-Ni(2)-N(2)	89.7(3)
O(4)-Ni(2)-O(11)	91.2(3)	O(4)-Ni(2)-N(3)	102.1(3)
O(12)-Ni(2)-O(11)	88.4(3)	O(12)-Ni(2)-N(3)	92.7(3)
O(6)-Ni(2)-O(11)	87.9(3)	O(6)-Ni(2)-N(3)	78.9(3)
O(4)-Ni(2)-N(2)	79.8(3)	O(11)-Ni(2)-N(3)	166.7(3)
O(12)-Ni(2)-N(2)	165.8(3)	N(2)-Ni(2)-N(3)	92.4(3)
O(14)-Ni(3)-O(19)#2	170.8(4)	O(22)-Ni(3)-N(5)	166.7(4)
O(14)-Ni(3)-O(22)	87.6(4)	O(21)-Ni(3)-N(5)	82.9(4)
O(19)#2-Ni(3)-O(22)	83.5(4)	O(14)-Ni(3)-N(8)#2	99.5(4)
O(14)-Ni(3)-O(21)	90.5(4)	O(19)#2-Ni(3)-N(8)#2	78.8(4)
O(19)#2-Ni(3)-O(21)	92.1(5)	O(22)-Ni(3)-N(8)#2	94.9(5)
O(22)-Ni(3)-O(21)	90.6(5)	O(21)-Ni(3)-N(8)#2	168.8(4)
O(14)-Ni(3)-N(5)	81.0(4)	N(5)-Ni(3)-N(8)#2	93.6(4)
O(19)#2-Ni(3)-N(5)	108.1(4)	O(15)-Ni(4)-O(18)	169.1(3)
O(15)-Ni(4)-N(7)	103.9(3)	N(7)-Ni(4)-N(6)	92.7(3)
O(18)-Ni(4)-N(7)	80.3(3)	O(24)-Ni(4)-N(6)	167.8(4)
O(15)-Ni(4)-O(24)	88.0(4)	O(15)-Ni(4)-O(23)	91.0(4)
O(18)-Ni(4)-O(24)	81.9(4)	O(18)-Ni(4)-O(23)	85.0(4)
N(7)-Ni(4)-O(24)	90.3(4)	N(7)-Ni(4)-O(23)	165.1(4)
O(15)-Ni(4)-N(6)	79.8(3)	O(24)-Ni(4)-O(23)	90.0(5)
O(18)-Ni(4)-N(6)	110.3(3)	N(6)-Ni(4)-O(23)	90.0(5)
O(26)#3-Ni(5)-O(26)#4	89.7(3)	O(26)-Ni(5)-O(25)#4	177.6(4)
O(26)#3-Ni(5)-O(26)	89.7(3)	O(25)#3-Ni(5)-O(25)#4	88.9(5)
O(26)#4-Ni(5)-O(26)	89.7(3)	O(26)#3-Ni(5)-O(25)	177.6(4)
O(26)#3-Ni(5)-O(25)#3	89.1(4)	O(26)#4-Ni(5)-O(25)	92.3(4)
O(26)#4-Ni(5)-O(25)#3	177.6(4)	O(26)-Ni(5)-O(25)	89.1(4)

O(26)-Ni(5)-O(25)#3	92.3(4)	O(25)#3-Ni(5)-O(25)	88.9(5)
O(26)#3-Ni(5)-O(25)#4	92.3(4)	O(25)#4-Ni(5)-O(25)	88.9(5)
O(26)#4-Ni(5)-O(25)#4	89.1(4)		

Symmetry transformations used to generate equivalent atoms: #1 -x+y+2, -x+1, z #2 -y+1, x-y-1, z #3 -x+y+2, -x+2, z #4 -y+2, x-y, z #5 -y, x-y, z #6 -x+y, -x, z

Complex 1^{SS}

Ni(1)-O(7)#1	2.047(7)	Ni(1)-O(2)	2.061(7)
Ni(1)-O(10)	2.056(8)	Ni(1)-N(4)#1	2.118(8)
Ni(1)-O(9)	2.058(9)	Ni(1)-N(1)	2.126(8)
Ni(2)-O(4)	2.013(7)	Ni(2)-N(3)	2.085(8)
Ni(2)-O(6)	2.049(8)	Ni(2)-N(2)	2.093(8)
Ni(2)-O(12)	2.067(8)	Ni(2)-O(11)	2.127(9)
Ni(3)-O(20)	2.004(8)	Ni(3)-O(22)	2.087(10)
Ni(3)-O(21)	2.039(11)	Ni(3)-N(8)	2.093(9)
Ni(3)-O(14)#4	2.042(7)	Ni(3)-N(5)#4	2.115(8)
Ni(4)-O(18)	2.029(9)	Ni(4)-O(23)	2.087(12)
Ni(4)-O(24)	2.046(12)	Ni(4)-N(7)	2.104(10)
Ni(4)-O(15)	2.045(8)	Ni(4)-N(6)	2.192(13)
Ni(5)-O(25)	2.025(13)	Ni(5)-O(26)	2.153(9)
Ni(5)-O(25)#5	2.025(13)	Ni(5)-O(26)#5	2.153(9)
Ni(5)-O(25)#6	2.025(13)	Ni(5)-O(26)#6	2.153(9)
O(7)#1-Ni(1)-O(10)	86.8(3)	O(9)-Ni(1)-N(4)#1	89.2(4)
O(7)#1-Ni(1)-O(9)	89.8(3)	O(2)-Ni(1)-N(4)#1	108.5(3)
O(10)-Ni(1)-O(9)	87.5(4)	O(7)#1-Ni(1)-N(1)	102.4(3)
O(7)#1-Ni(1)-O(2)	171.7(3)	O(10)-Ni(1)-N(1)	92.7(4)
O(10)-Ni(1)-O(2)	85.0(3)	O(9)-Ni(1)-N(1)	167.8(3)
O(9)-Ni(1)-O(2)	88.6(4)	O(2)-Ni(1)-N(1)	79.3(3)
O(7)#1-Ni(1)-N(4)#1	79.6(3)	N(4)#1-Ni(1)-N(1)	93.3(3)
O(10)-Ni(1)-N(4)#1	166.1(3)	O(4)-Ni(2)-O(6)	171.1(3)
O(4)-Ni(2)-O(12)	84.0(3)	O(12)-Ni(2)-N(2)	94.5(4)
O(6)-Ni(2)-O(12)	87.2(3)	N(3)-Ni(2)-N(2)	95.3(3)
O(4)-Ni(2)-N(3)	109.7(3)	O(4)-Ni(2)-O(11)	87.2(3)
O(6)-Ni(2)-N(3)	78.9(3)	O(6)-Ni(2)-O(11)	91.2(4)
O(12)-Ni(2)-N(3)	164.5(3)	O(12)-Ni(2)-O(11)	88.1(4)
O(4)-Ni(2)-N(2)	78.9(3)	N(3)-Ni(2)-O(11)	85.4(3)
O(6)-Ni(2)-N(2)	103.2(3)	N(2)-Ni(2)-O(11)	165.4(4)
O(20)-Ni(3)-O(21)	90.2(5)	O(14)#4-Ni(3)-N(8)	109.3(3)
O(20)-Ni(3)-O(14)#4	169.5(3)	O(22)-Ni(3)-N(8)	168.5(4)
O(21)-Ni(3)-O(14)#4	86.7(5)	O(20)-Ni(3)-N(5)#4	103.6(3)
O(20)-Ni(3)-O(22)	87.7(4)	O(21)-Ni(3)-N(5)#4	165.9(4)
O(21)-Ni(3)-O(22)	86.6(6)	O(14)#4-Ni(3)-N(5)#4	79.2(3)
O(14)#4-Ni(3)-O(22)	82.2(4)	O(22)-Ni(3)-N(5)#4	90.6(4)
O(20)-Ni(3)-N(8)	80.8(3)	N(8)-Ni(3)-N(5)#4	92.5(3)
O(21)-Ni(3)-N(8)	92.9(5)	O(18)-Ni(4)-O(24)	91.9(4)
O(18)-Ni(4)-O(15)	171.2(4)	O(15)-Ni(4)-N(7)	108.6(4)
O(24)-Ni(4)-O(15)	89.7(5)	O(23)-Ni(4)-N(7)	166.9(4)
O(18)-Ni(4)-O(23)	88.3(4)	O(18)-Ni(4)-N(6)	100.7(4)
O(24)-Ni(4)-O(23)	87.9(6)	O(24)-Ni(4)-N(6)	167.2(4)
O(15)-Ni(4)-O(23)	83.1(4)	O(15)-Ni(4)-N(6)	78.3(4)
O(18)-Ni(4)-N(7)	80.2(4)	O(23)-Ni(4)-N(6)	94.7(5)
O(24)-Ni(4)-N(7)	86.3(5)	N(7)-Ni(4)-N(6)	93.6(4)

O(25)#5-Ni(5)-O(25)#6	92.0(6)	O(25)-Ni(5)-O(26)#5	178.3(5)
O(25)#5-Ni(5)-O(25)	92.0(6)	O(26)-Ni(5)-O(26)#5	89.7(3)
O(25)#6-Ni(5)-O(25)	92.0(6)	O(25)#5-Ni(5)-O(26)#6	178.3(5)
O(25)#5-Ni(5)-O(26)	89.6(6)	O(25)#6-Ni(5)-O(26)#6	88.7(5)
O(25)#6-Ni(5)-O(26)	178.3(5)	O(25)-Ni(5)-O(26)#6	89.6(6)
O(25)-Ni(5)-O(26)	88.7(5)	O(26)-Ni(5)-O(26)#6	89.7(3)
O(25)#5-Ni(5)-O(26)#5	88.7(5)	O(26)#5-Ni(5)-O(26)#6	89.7(3)
O(25)#6-Ni(5)-O(26)#5	89.6(6)		

Symmetry transformations used to generate equivalent atoms: #1 -x+y+1, -x+2, z #2 -y+2, x-y+1, z #3 -y+1, x-y-1, z #4 -x+y+2, -x+1, z #5 -x+y+1, -x+1, z #6 -y+1, x-y, z

References

- [1]. M. L. Baker, T. Lancaster, A. Chiesa, G. Amoretti, P. J. Baker, C. Barker, S. J. Blundell, S. Carretta, D. Collison, H.U. Güdel, *Chem.A Eur. J.* **2016**, 22, 1779.
- [2]. P. L. Polavarapu, *Chiroptical spectroscopy: Fundamentals and applications*, Crc Press, **2016**.
- [3]. M. Bilal, H. M. Iqbal, H. Hu, W. Wang, X. Zhang, *Sci. Total Environ.* **2017**, 575, 1352.
- [4]. (a) Zhang, L.; Wei, Y.; Wang, C.; Guo, H.; Wang, P. J. *Solid State Chem.* **2004**, 177, 3433. (b) Liao, J. H.; Juang, J. S.; Lai, Y. C. *Cryst. Growth Des.* 2006, 6, 354. (c) Xia, Y.; Wu, P. F.; Wei, Y. G.; Wang, Y.; Guo, H. Y. *Cryst. Growth Des.* **2006**, 6, 253.
- [5]. SMART-CCD Software, version 5.0; Siemens Analytical X-ray Instruments: Madison, WI, **1996**.
- [6]. G. M. Sheldrick, SHELXT-Integrated space-group and crystal structure determination. *Acta Crystallogr.* **2015**, A71, 3.
- [7]. G.M. Sheldrick, Crystal structure refinement with SHELXL, *Acta Crystallogr.* **2015**, C71, 3.
- [8]. A. L. Sepek, *Acta. Cryst.***2009**, D65, 148.